ELSEVIER

Materials Science and Engineering A 419 (2006) 357–364

MATERIALS SCIENCE & ENGINEERING A

www.elsevier.com/locate/msea

Effect of volume fraction and particle size on the microstructure and plastic deformation of Mg–Y_2O_3 composites

G. Garcés *, M. Rodríguez, P. Pérez, P. Adeva

Department of Physical Metallurgy, National Centre for Metallurgical Research CENIM-CSIC, Av. Gregorio del Amo 8, 28040 Madrid, Spain

Received 8 April 2005; received in revised form 12 January 2006; accepted 13 January 2006

Abstract

The plastic behaviour at room temperature of magnesium and magnesium metal matrix composites reinforced with yttria particles of two sizes is studied. All the materials are produced by powder metallurgy. During extrusion both the unreinforced magnesium and the composites develop a fibre texture with the $\{1\,0\,\bar{1}\,0\}$ planes perpendicular to the extrusion direction. The fibre intensity decreases as the volume fraction of yttria particles increases. A tension/compression asymmetry is observed. The extrusion texture prevents deformation by the basal slip system in both tension and compression. Deformation in the $\{1\,0\,\bar{1}\,2\}\langle 1\,0\,\bar{1}\,1\rangle$ twinning system is only possible in compression. As the volume fraction of yttria particles increases, the texture becomes more random and the tension/compression asymmetry tends to decrease and is eventually reversed. The composites reinforced with the smallest ceramic particles present the highest yield stress.
© 2006 Elsevier B.V. All rights reserved.

Keywords: Magnesium; Metal matrix composites (MMC); Plastic deformation

1. Introduction

Magnesium alloys present great potential as structural materials in the aerospace and automobile industries, mainly because of their low density and high specific strength. However, due to their rapid loss of strength at temperatures above room temperature and their poor creep resistance at high temperatures, magnesium alloys are rarely used above 200 °C. The addition of stiffer phases such as ceramic or metallic particles [1–9], ceramic short-fibres [10–15] or carbon fibres [16–18] to magnesium alloys improves their high temperature creep resistance and leads to an increase in their tensile strength, Young's modulus, hardness (particularly at room temperature) and wear resistance.

An important aspect of magnesium alloys is their anisotropy. The mechanical properties of these materials are strongly dependent on their texture, especially at low temperature. Wrought magnesium alloys develop a strong texture with the basal plane perpendicular to the deformation direction [19–21], and their mechanical properties thus depend not only on the stress direction but also on the stress sign (tension or compression) [21]. The tension/compression asymmetry at room temperature is a well-known phenomenon in wrought magnesium alloys and is related to their texture, which determines the slip and twinning systems controlling plastic flow. The systems most easily activated at room temperature are $(0\,0\,0\,1)\langle 1\,1\,\bar{2}\,0\rangle$ basal slip and $\{1\,0\,\bar{1}\,2\}\langle 1\,0\,\bar{1}\,1\rangle$ twinning [22–27]. However, the basal slip system is inhibited when the material is deformed in the extrusion or rolling direction and the $\{1\,0\,\bar{1}\,2\}\langle 1\,0\,\bar{1}\,1\rangle$ twinning system is active in compression but not in tension.

The addition of ceramic reinforcement reduces the intensity of the crystallographic texture created during deformation processing because of the complex deformation pattern around the hard ceramic particles [28–30]. It has recently been observed that the addition of ceramic particles induces a decrease in the $\{1\,0\,\bar{1}\,0\}$ fibre texture developed during extrusion and thus a decrease in the tension/compression asymmetry when the composite is deformed in the extrusion direction [31].

The present study has been carried out to investigate the deformation behaviour of magnesium metal matrix composites reinforced with Y_2O_3 ceramic particles of two different sizes. Tension and compression tests have been performed to correlate mechanical anistropy with texture, quantifying the contributions of basal slip and pyramidal $\{1\,0\,\bar{1}\,2\}\langle 1\,0\,\bar{1}\,1\rangle$ twinning. For comparative purposes, unreinforced magnesium has also been studied.

* Corresponding author. Tel.: +34 915538900; fax: +34 915347425.
E-mail address: ggarces@cenim.csic.es (G. Garcés).

0921-5093/$ – see front matter © 2006 Elsevier B.V. All rights reserved.
doi:10.1016/j.msea.2006.01.026

2. Experimental procedure

Commercial magnesium powders of less than 45 μm in size were blended with 5, 10, 15 and 20% volume of Y_2O_3 particles of two different sizes: 6 and <1 μm. Blend homogenisation was conducted in a high speed impeller at 110 rpm for 4 h in an air atmosphere. After homogenisation the powders were cold compacted by slowly increasing the pressure up to 310 MPa. Compacts of 40 mm in diameter were extruded at 400 °C employing an extrusion ratio of 18:1.

Microstructural characterisation of the composites was carried out by X-ray diffraction and optical and electron microscopy. Metallographic preparation for SEM observation consisted of mechanical polishing and etching in a solution of 5 g of picric acid, 5 ml of water and 25 ml of ethanol. X-ray diffraction was used for texture measurements. Texture analysis was performed by the Schulz reflection method, using a SIEMENS TM Kristalloflex D5000 diffractometer equipped with a Eulerian cradle. The X-radiation used was β-filtered Cu Kα. The orientation distribution functions (ODFs) were computed from the measurement of (0 0 0 2), $\{1\,0\,\bar{1}\,1\}$, $\{1\,0\,\bar{1}\,2\}$, $\{1\,0\,\bar{1}\,3\}$ and $\{1\,1\,\bar{2}\,0\}$ pole figures by the series expansion method. The reference system was selected with the *Z*-axis parallel to the extrusion direction.

Young's modulus and Poisson ratio measurements were carried out by ultrasonic phase spectroscopy. The frequency range used in the experiments was between 10 kHz and 10 GHz.

Hardness and tensile and compressive tests were carried out to evaluate the mechanical properties of the unreinforced magnesium and the composites. Vickers hardness measurements were performed by applying 49.05 N for 15 s in the extrusion and normal directions. Cylindrical samples (head diameter 6 mm, curvature radius 3 mm, gauge diameter 3 mm and gauge length 10 mm) for tensile tests and cylinders (diameter 7.5 mm and length 15 mm) for compressive tests were machined from the extruded bar with the longer dimension parallel to the extrusion direction. Tensile and compressive tests were performed in a universal tensile machine with constant cross-head speed at an initial strain rate of $10^{-4}\ s^{-1}$ at room temperature. BN was used as lubricant in the compressive tests in order to prevent barrelling.

Table 1
Grain size of unreinforced magnesium and composites

Y_2O_3 (%)	$D < 1$ μm	$D = 6$ μm
5	2.99 ± 0.1	2.49 ± 0.1
10	1.67 ± 0.07	1.93 ± 0.07
15	1.23 ± 0.03	1.24 ± 0.03
20	1.17 ± 0.04	1.16 ± 0.03
Mg	7.14 ± 1.03	

3. Results

3.1. Microstructural characterisation

The microstructure of the original magnesium powders (Fig. 1(a)) experiences substantial grain growth during the subsequent extrusion process (Fig. 1(b)). Grains are elongated in the extrusion direction and the grain size is heterogeneous. During extrusion the oxide layer covering the original powder is broken and small oxide particles appear decorating the particle boundaries.

Fig. 2(a–h) shows the microstructure of the composites. The white and grey phases correspond to the yttria particles and magnesium matrix, respectively. The yttria particle distribution depends on the particle size and volume fraction. Progressive agglomeration of the yttria particles occurs as the reinforcement volume fraction increases. This phenomenon is especially noticed with particles smaller than 1 μm.

Table 1 presents the grain size values recorded for unreinforced magnesium and the composites by image analysis. As is common in composite materials, the grain size decreases as the ceramic particle volume fraction rises. Since yttria and magnesia particles act as nucleation sites for recrystallised grains during extrusion, the volume fraction of recrystallised grains also rises when the reinforcement volume fraction is increased. It is interesting to note the negligible influence of the yttria particle size on the composite grain size.

Texture is evaluated to determine the effect of the yttria particle size and volume fraction on the grain orientation. For comparative purposes the extruded pure magnesium was

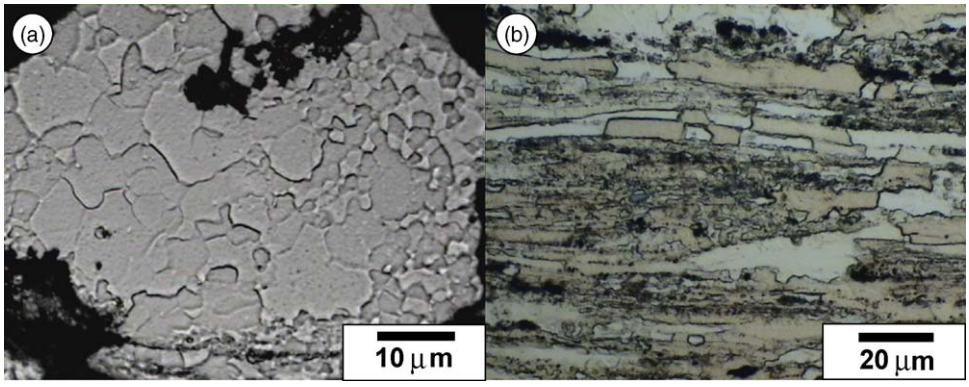


Fig. 1. Micrographs showing the grain structure distribution of: (a) magnesium powder and (b) unreinforced magnesium after extrusion at 400 °C.

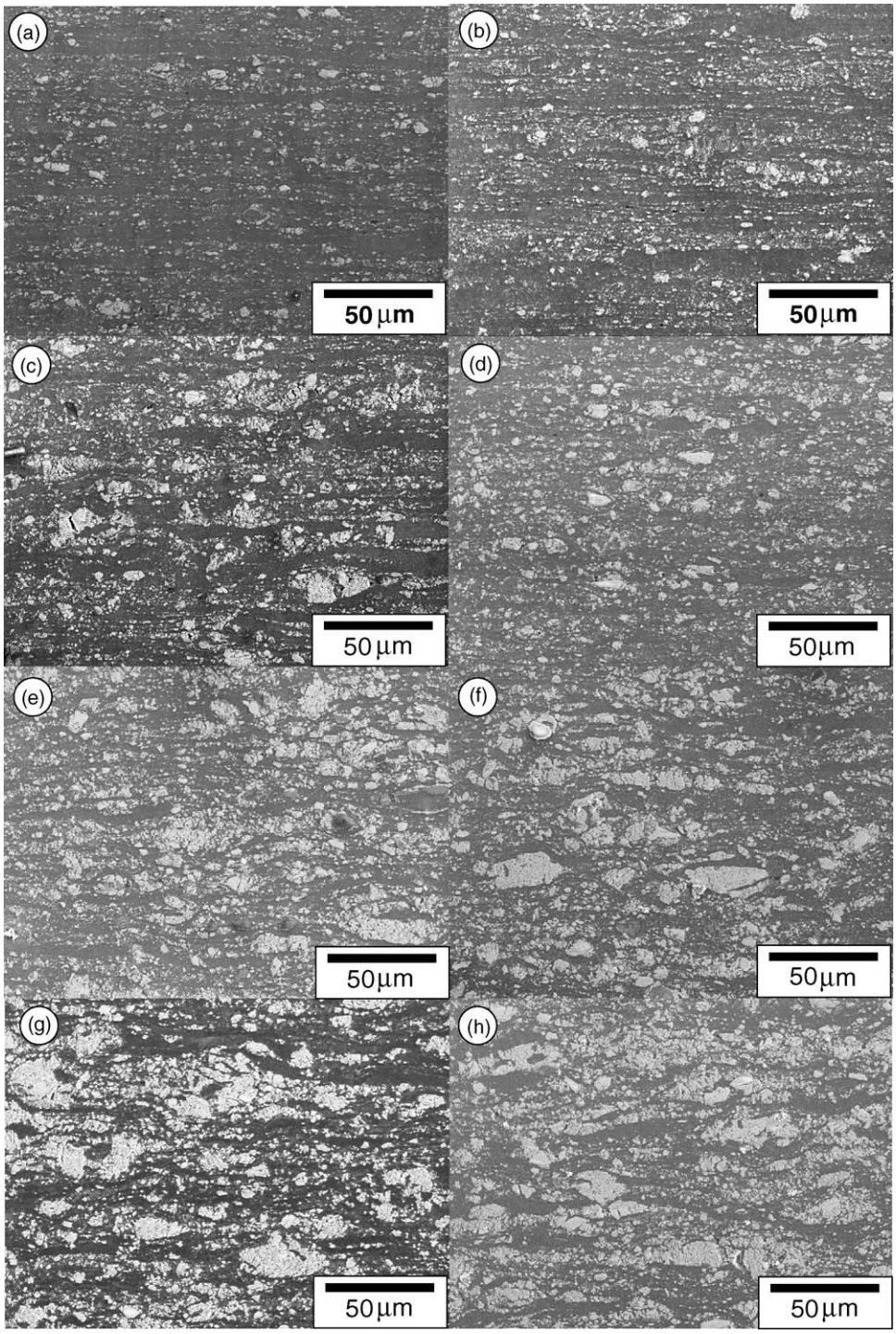


Fig. 2. Composite microstructure in the extrusion direction: (a) Mg–5% Y_2O_3 (<1 μm); (b) Mg–5% Y_2O_3 (6 μm); (c) Mg–10% Y_2O_3 (<1 μm); (d) Mg–10% Y_2O_3 (6 μm); (e) Mg–15% Y_2O_3 (<1 μm); (f) Mg–15% Y_2O_3 (6 μm); (g) Mg–20% Y_2O_3 (<1 μm); (h) Mg–20% Y_2O_3 (6 μm). The white and dark phases correspond to the reinforcement and matrix, respectively.

also studied. All the materials show the typical extrusion texture of magnesium alloys with the basal plane parallel to the extrusion direction. Fig. 3(a and b) shows the intensity of the $(0\,0\,0\,2)$ and $(1\,0\,\bar{1}\,0)$ pole figures as a function of the polar angle. Although the texture is similar in all the materials, the fibre intensity decreases as the reinforcement volume fraction increases.

3.2. Mechanical characterisation

Fig. 4 shows the Young modulus values measured in the extrusion direction. The Young modulus increases with the ceramic particle volume fraction. The Poisson ratio was also measured and is seen to remain constant (around 0.31) irrespective of the yttria addition.

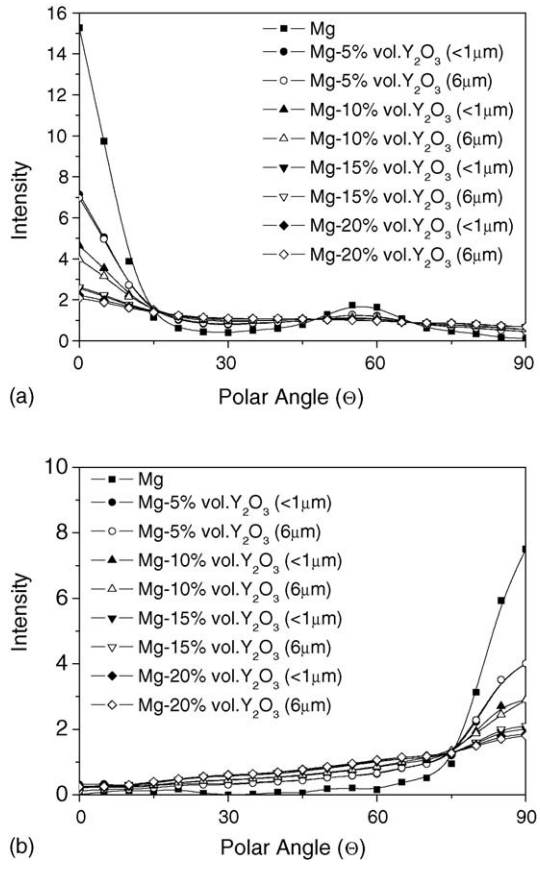


Fig. 3. Pole figure intensity of: (a) $\{1\,0\,\bar{1}\,0\}$ and (b) $\{0\,0\,0\,2\}$ planes as a function of the polar angle (Θ).

Fig. 5 plots the evolution of hardness, which increases linearly with the yttria particle volume fraction. Hardness values are similar for both reinforcement particle sizes; except in the case of magnesium reinforced with 20% of yttria particles, where the hardness is lower with <1 μm particles than with 6 μm particles.

Fig. 6(a) shows tensile and compressive curves for unreinforced magnesium and the composites reinforced with 10 and 20% (vol.%) of 6 μm yttria particles. Fig. 6(b) also summarises

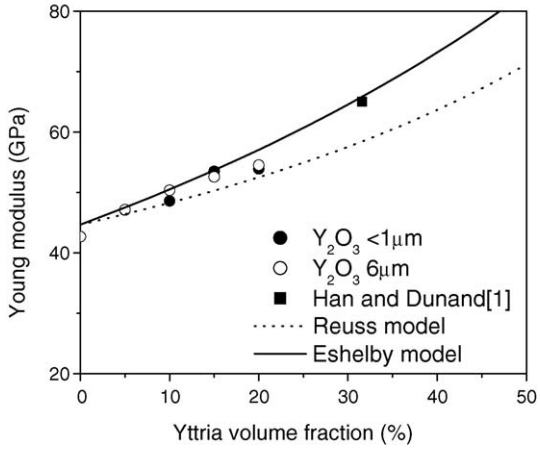


Fig. 4. Young modulus of unreinforced magnesium and composites. The data are compared with the Reuss and Eshelby models.

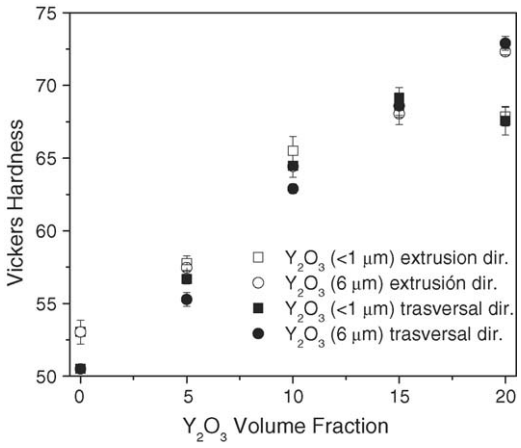


Fig. 5. Composite hardness evolution as a function of yttria volume fraction.

the yield stress values obtained in tensile and compressive tests as a function of the yttria particle size and volume fraction. Table 2 shows the elongation to failure (in tension) of the unreinforced magnesium and the composites. In tensile behaviour, yield stress and elongation to failure decrease continuously as the volume fraction of yttria particles rises. Furthermore, the Mg–20% Y_2O_3 with submicron yttria particles failed in the elastic regime, preventing the determination of yield and ultimate tensile stresses. The yield stress of the composite reinforced with <1 μm particles is always higher than that of the composite reinforced with coarser yttria particles.

In compression, plastic behaviour is completely different and yield stress increases with the yttria volume fraction. Similarly to the case of tension, the yield stress is higher with submicrometric yttria particles, except for the composite reinforced with a 20% volume fraction of submicron yttria particles. With unreinforced magnesium, the stress reaches a maximum close to the yield stress and then decreases to a minimum at a strain of around 2.5%. After this minimum, strain hardening increases again constantly up to fracture. As the ceramic particle volume fraction increases, work hardening decreases as compared to the unreinforced magnesium, as can be seen in Fig. 6(a).

Finally, a tension/compression asymmetry is clearly observed with both unreinforced and reinforced materials (Fig. 6). This effect is common in magnesium alloys where tension is always stronger than compression. However, the asymmetry ratio for the composites, defined as $\sigma_{0.2}^{ten}/\sigma_{0.2}^{com}$, decreases as the yttria volume fraction drops (Fig. 7). For yttria volume fractions of more than 15%, the yield stress is higher in compression than in tension.

Table 2
Elongation to failure of unreinforced magnesium and composites

Y_2O_3 (%)	$D<1$ μm (%)	$D=6$ μm (%)
5	4	3.5
10	2	1.8
15	1	1.1
20	0	0.2
Mg	3	

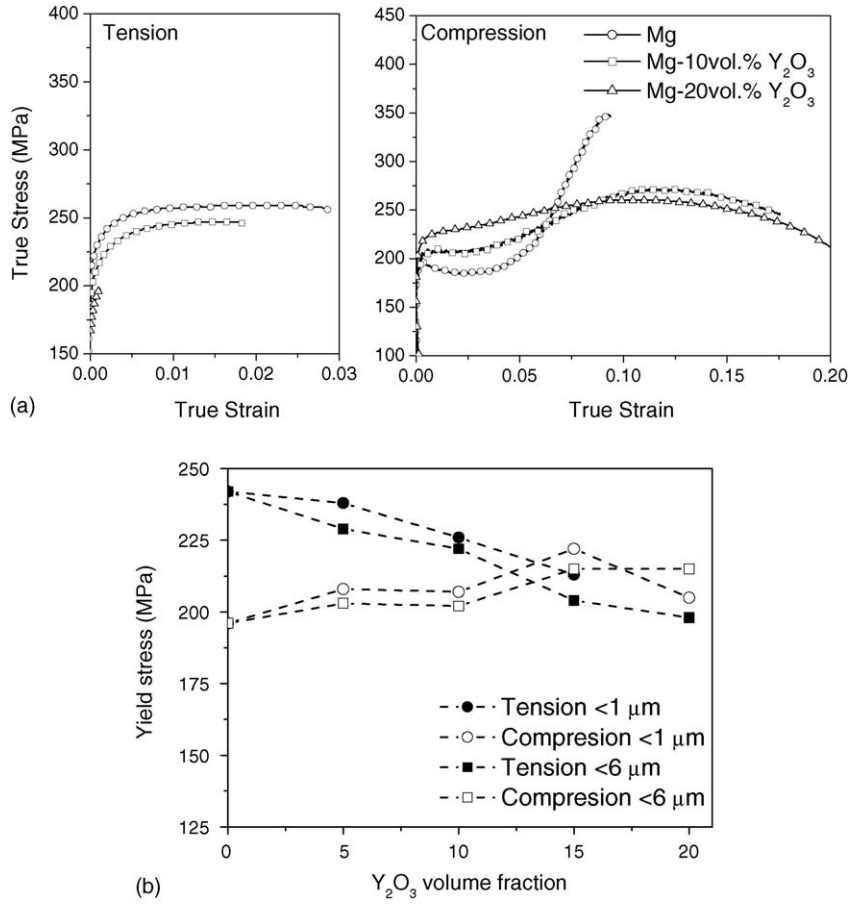


Fig. 6. (a) Tensile and compressive stress–strain curves for extruded magnesium and composites with a particle volume fraction of: (a) 5% and (b) 10% (particle size 6 μm). (b) Yield stress and maximum strength of extruded magnesium and composites for tension and compression.

In the entire reinforcement volume fraction range, except for the Mg–20% Y_2O_3 composite, the fracture surface of tensile tested samples at room temperature shows ductile transgranular failure through the magnesium matrix (Fig. 8(a)) and a large amount of microvoids in the magnesium matrix is observed. In contrast, with the Mg–20% Y_2O_3 composite the fracture occurs in the elastic regime and is caused by the presence of yttria agglomerates (Fig. 8(b)).

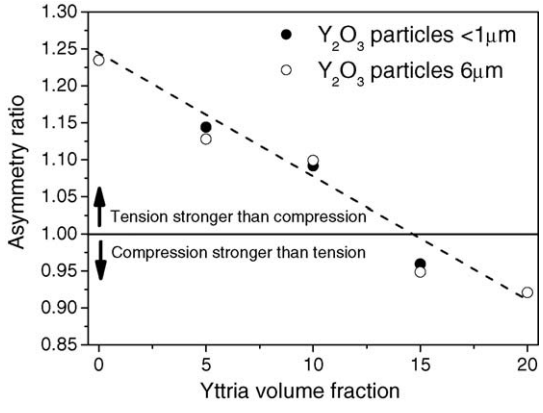


Fig. 7. Asymmetry ratio, $\sigma_{0.2}^{ten}/\sigma_{0.2}^{com}$, for unreinforced magnesium and composite materials.

4. Discussion

Although the unreinforced and composite materials develop qualitatively similar deformation textures in the matrix, the intensity of the fibre texture intensity varies with yttria volume fraction. This phenomenon has also been reported for aluminium matrix composites [28–30]. It is suggested that particle stimulated nucleation for recrystallisation (PSN) at the Y_2O_3–Mg interfaces may be responsible for a certain randomisation of texture in the composite matrix grains. The occurrence of this phenomenon agrees with the more equiaxed grain structure and the smaller grain size of these composites compared to the unreinforced alloy. In fact, the progressive increase in the volume fraction of yttria particles may inhibit the development of the strong $\{1\,0\,\bar{1}\,0\}$ fibre texture.

The Young modulus increases with the ceramic particle volume fraction. Fig. 4 shows the evolution of Young modulus with yttria volume fraction. For comparison, the elastic modulus of the composite materials is calculated according to the Reuss and Eshelby models [32], with the elastic modulus and Poisson ratio of magnesium and yttria given as $E_{Mg} = 44.7$ GPa, $\nu_{Mg} = 0.35$ and $E_{Yttria} = 177$ GPa, $\nu_{yttria} = 0.30$, respectively [1]. The Reuss model underestimates the measured Young modulus values while the Eshelby model agrees fairly well with the exper-

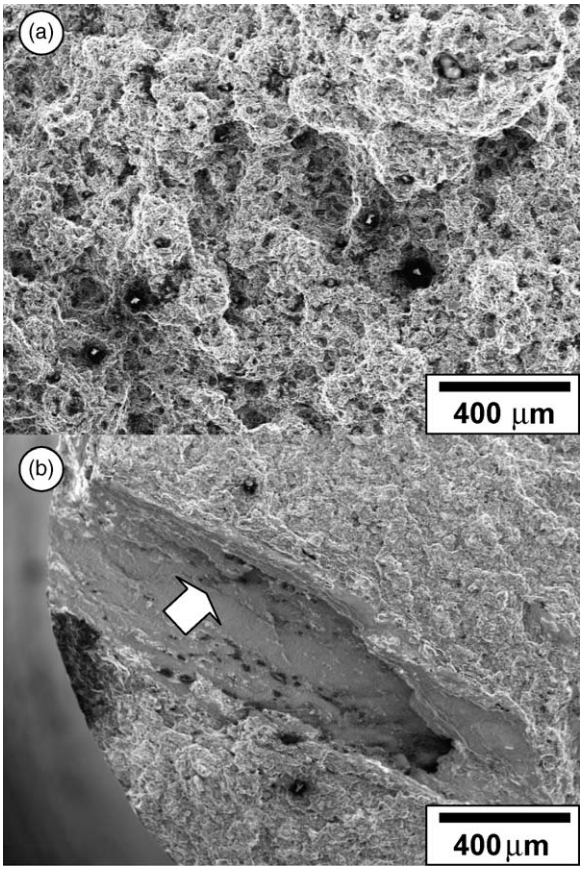


Fig. 8. Fracture surface of: (a) unreinforced magnesium and (b) Mg–20% Y_2O_3 (<1 μm). The white arrow points to an yttria agglomeration that causes brittle fracture.

imental data obtained for the extruded Mg–Y_2O_3 composites in this work.

As mentioned in Section 3, the addition of a hard ceramic phase to the magnesium matrix produces an increase in hardness. Magnesium is a very anisotropic material and its mechanical properties depend strongly on its texture. This anisotropy is also reflected in the hardness values of the unreinforced magnesium, which is stronger in the extrusion direction than in the transversal direction (Fig. 5). These differences between the two directions tend to disappear as the ceramic particle volume fraction increases. This asymmetry is also clearly observed in the tensile/compressive tests.

In tension the composite yield stress decreases with the ceramic particle volume fraction irrespective of the ceramic particle size. At room temperature, basal slip is the only slip system in the magnesium. For the unreinforced magnesium, which develops a strong $\{1\,0\,\bar{1}\,0\}$ fibre texture, the basal slip system is inhibited in most of the grains when the material is deformed in the extrusion direction. Thus, the more intense the $\{1\,0\,\bar{1}\,0\}$ fibre texture, the higher the yield stress. This explains the higher yield stress observed in unreinforced magnesium than in the composite materials. As the volume fraction increases, the texture continuously decreases and there are more grains favourably oriented for basal slip.

On the other hand, in contrast to this tensile behaviour, the composite yield stress in compression increases with the ceramic particle volume fraction. In compression, twinning in the $\{1\,0\,\bar{1}\,2\}\langle 1\,0\,\bar{1}\,1\rangle$ system takes place and the unreinforced magnesium and composites with a low yttria volume fraction yield at a lower stress than in tension [22–24].

The increase in work hardening in unreinforced magnesium during compression arises as a consequence of twinning. There are some explanations which can rationalize this effects: (i) twinning introduces additional barriers to dislocation movements [33] which are equivalent to a grain size reduction, (ii) $\{1\,0\,\bar{1}\,2\}\langle 1\,0\,\bar{1}\,1\rangle$ twinning in magnesium induces a lattice reorientation which is also not good oriented for basal slip [19,26] and (iii) the transformation of dislocations as they pass trough the twinning front can lead to the establishment of high hardening rates within the twin interior [34]. Recent results [27] have shown that reasons (ii) and (iii) are probably the main reasons for the high degree of hardening due to twinning.

As the yttria volume fraction increases, work hardening during compression decreases. Barnett et al. have observed in magnesium alloys that for fine grains twinning is inhibited [27]. Furthermore, as the composite texture becomes random for a higher reinforcement volume fraction, plastic deformation proceeds progressively by dislocation slip. Therefore, the decrease in the dislocation–twinning interaction leads to a decrease in work hardening.

The contribution of the presence of yttria particles to yield stress is due to a number of different mechanisms:

- *Orowan mechanism*: The interaction between dislocations and fine particles results in an increase in yield stress. However, this mechanism is only effective in the case of ODS materials when the second phase particles are mainly located within grains. In the studied composites, the ceramic particles are mainly located at the grain boundaries and the reinforcement effect due to the Orowan mechanism will therefore be minor. It is also interesting to note that the particles are too coarse to contribute to the Orowan mechanism, even if the particles are not at the grain boundaries.
- *CTE mismatch*: Dislocations are created from the relaxation of the thermal expansion mismatch between the matrix and the reinforcement particles and may cause an increase in the yield stress which is expressed as:

$$\sigma^{\mathrm{CTE}} = AMGb\sqrt{\rho}, \tag{1}$$

where $M = 6.5$ [35] is the mean matrix orientation factor for magnesium and the constant $A = 0.2$ characterises the transparency of the dislocation forest for basal–basal dislocations in magnesium at room temperature [36]. The Burgers vector and the shear modulus are taken as $b = 3.21 \times 10^{-10}$ m and $G = 16.6$ Gpa [37], respectively. The dislocation density can be estimated by assuming that dislocation loops of radius $d/\sqrt{2}$ are punched by spherical particles with a volume fraction f to

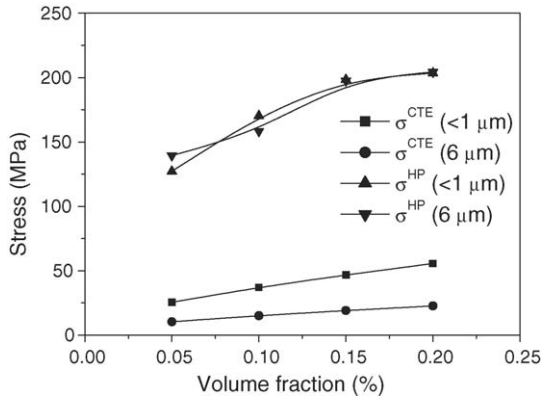


Fig. 9. Evolution of stress due to grain refinement (σ_{HP}) and increases in dislocation density because of differences in CTE between the matrix and ceramic particles (σ_{CTE}) as a function of the yttria volume fraction and particle size.

relax the thermal expansion coefficients $\Delta\alpha$ [1]:

$$\rho^{CTE} = \frac{12\sqrt{2}\Delta\alpha\Delta T f}{bd(1-f)} \quad (2)$$

The average thermal expansion coefficients of pure magnesium and yttria are 2.7×10^{-5} and $7.5\times10^{-6}\,K^{-1}$, respectively. Taking $\Delta T = 250\,K$ (corresponding to the stress-free homologous temperature of 0.6), Fig. 9 shows the increment of the yield stress due to the presence of dislocations produced by the difference between the thermal expansion coefficients of the matrix and the yttria particles. σ^{CTE} increases with the ceramic particle volume fraction and with the decrease in particle size. This would explain the higher yield stresses observed in the composites reinforced with submicrometric yttria particles.

- *Grain size refinement:* As the ceramic volume fraction rises, the composite grain size diminishes (Table 1), causing strengthening by the Hall–Petch mechanism. The particles control the grain size in the metal matrix composites since they prevent grain growth. This fact has clearly been observed in the microstructure of the composites, where the ceramic particles are located at the grain boundaries. The Hall–Petch relation is described by [38]:

$$\sigma^{HP} = \sigma_0 + \frac{K}{\sqrt{D}}, \quad (3)$$

where σ_0 is the friction stress, D the grain size and K is a constant. For pure magnesium, the K value depends on the stress direction, i.e. tension or compression [39,40]. We have used $K = 0.22\,MPa\,m^{-1/2}$, obtained for hot extruded Mg by Hauser et al. [39]. Fig. 9 shows the grain size contribution to the composite strength obtained from Eq. (3) using experimental composite grain size values (Table 1). Since no grain size differences were observed between the two yttria particle sizes, similar σ^{HP} values have been predicted by Eq. (3).
- *Residual stresses*: In composite materials, the presence of residual stress due to differences between the thermal expansion coefficients of the ceramic particles and the metallic matrix has been reported. The matrix remains in tension and the reinforced phase in compression. In aluminium matrix composites, the yield stress is higher in tension than in compression (strength differential effect) [41]. This fact may explain the tension/compression asymmetry evolution for higher ceramic particle volume fractions (Fig. 6(b)). When the texture is random, its contribution to the composite yield stress disappears and the residual stresses seem to induce a higher yield stress in compression than in tension.

It is possible to conclude from the tension and compression results that the yield stress in the extruded magnesium composites has three main contributions: the strong extrusion texture, grain refinement and the increases in dislocation density due to CTE mismatch between the matrix and the ceramic particles.

In tension and compression, the texture contribution decreases progressively with the yttria volume fraction due to the decrease in the $\{1\,0\,\bar{1}\,0\}$ fibre intensity. However, the negative slope is steeper in tension than in compression, because in compression at least twinning is possible. On the other hand, the reinforcement effect due to grain refinement and the increase in dislocation density may be assumed to be similar in both tension and compression and to increase with the ceramic volume fraction (Fig. 9). Taking into account the three effects, the yield stress general tendency is the reverse in tension to in compression, i.e. decreases in tension and increases in compression, and for higher ceramic particle volume fractions the composites become stronger in compression than in tension.

5. Conclusions

The effect of the addition of hard ceramic particles on the microstructure and mechanical properties of pure magnesium has been investigated. The following conclusions may be drawn:

1. The ceramic particles are more homogeneously distributed at lower volume fractions. In the case of higher volume fractions, the occurrence of particle agglomeration results in catastrophic mechanical failure.
2. The materials develop a fibre texture, with the $\{1\,0\,\bar{1}\,0\}$ planes perpendicular to the extrusion direction, whose intensity decreases as the volume fraction of yttria particles rises. The texture intensity determines the mechanical behaviour of the materials.
3. The yield stress of the extruded magnesium composites is comprised of three contributions: a strong extrusion texture; grain refinement; and an increase in the dislocation density due to CTE mismatch between the matrix and the ceramic particles. The predominant contribution of texture to the strength results in tensile yielding at higher stresses for the non-reinforced material. As the ceramic volume fraction increases, the texture becomes random and this effect tends to disappear.
4. As the reinforcement volume fraction increases, the refinement of grain size and increases in the dislocation density due to CTE mismatch come to control the composite strength. In fact, for higher yttria volume fraction increases, the asymmetry between tension and compression is reversed.

Acknowledgements

The authors (G.G.) would like to thank to the Ministry of Science and Technology for a contract within the Ramon y Cajal Programme. We gratefully acknowledge the support of the CAM 07N0075-2002. The authors would also like to thank Prof. Alexander Wanner for helping in the experiments and for discussing the phase spectroscopy results.

References

[1] B.Q. Han, D.C. Dunand, Mater. Sci. Eng. A 277 (2000) 297–304.
[2] B.Q. Han, D.C. Dunand, Mater. Sci. Eng. A 300 (2001) 235–244.
[3] P. Pérez, G. Garcés, P. Adeva, Comp. Sci. Technol. 64 (2004) 145–151.
[4] J. Lan, Y. Yang, X.C. Li, Mater. Sci. Eng. A 386 (2004) 284–290.
[5] C.Y.H. Lin, S.C. Lim, A. Gupta, Wear 255 (2003) 629–637.
[6] Q.C. Jiang, H.Y. Wang, B.X. Ma, Y. Wang, F. Zhao, J. Alloys Compd. 386 (2005) 177–181.
[7] S.F. Hassan, M. Gupta, Mater. Sci. Technol. 19 (2003) 253–259.
[8] X.N. Zhang, D. Zhang, R.J. Wu, Z.G. Zhu, C. Wang, Scr. Mater. 37 (1997) 1631–1635.
[9] H. Ferkel, B.L. Mordike, Mater. Sci. Eng. A 298 (2001) 193–199.
[10] K.U. Kainer, Mater. Sci. Eng. A 135 (1991) 243–246.
[11] V. Sklenicka, M. Pahutova, K. Kucharova, M. Svoboda, T.G. Langdon, Metall. Mater. Trans. A 33 (2002) 883–889.
[12] V. Sklenicka, M. Svoboda, M. Pahutova, K. Kucharova, T.G. Langdon, Mater. Sci. Eng. A 319 (2001) 741–745.
[13] C. Mayencourt, R. Schaller, Mater. Sci. Eng. A 325 (2002) 286–291.
[14] Y. Park, K. Terasaki, K. Igarashi, T. Shimizu, Adv. Comp. Mater. 10 (2001) 17–28.
[15] J.H. Gu, X.N. Zhang, M.Y. Gu, Mater. Trans. 45 (2004) 1743–1747.
[16] S. Vaucher, O. Beffort, J. Kubler, F. Lehner, Adv. Eng. Mater. 5 (2003) 669–672.
[17] H.P. Degischer, F.G. Rammerstorfer, O. Beffort, in: K.U. Kainer (Ed.), Magnesium Alloys and their Applications, Wiley-VHC, Weinheim, 2003, pp. 208–214.
[18] O. Beffort, C. Hausmann, in: K.U. Kainer (Ed.), Magnesium Alloys and their applications, Wiley-VHC, Weinheim, 2003, pp. 215–220.
[19] S.R. Agnew, M.H. Yoo, C.N. Tomé, Acta Mater. 49 (2001) 4277.
[20] A.D. Rollet, S.I. Wright, Texture and Anisotropy, University Press, Cambridge, 1998, p. 179.
[21] S. Kleiner, P.J. Uggowitzer, Mater. Sci. Eng. A 379 (2004) 258–263.
[22] B.C. Wonsiewicz, W.A. Backofen, Trans. Metall. Soc. AIME 239 (1967) 1422–1431.
[23] E.W. Kelley, W.F. Hosford, Trans. AIME 242 (1968) 5–13.
[24] E.W. Kelley, W.F. Hosford, Trans. AIME 242 (1968) 242–250.
[25] J.W. Christian, S. Mahajan, Prog. Mater. Sci. 39 (1995) 1–157.
[26] M.D. Nave, M.R. Barnett, Scr. Mater. 51 (2004) 881–885.
[27] M.R. Barnett, Z. Keshavarz, A.G. Beer, D. Atwell, Acta Mater. 52 (4) (2004) 5093–5103.
[28] F.J. Humphreys, W.S. Miller, M.R. Djazed, Mater. Sci. Technol. 6 (1990) 1157–1163.
[29] Y.L. Liu, N. Hansen, D.J. Jensen, Metal Matrix Composites—Processing, Microstructure and Properties, Risø, 1991, pp. 67–80.
[30] A.W. Bowen, M. Ardakani, F.J. Humphreys, Metal Matrix Composites—Processing, Microstructure and Properties, Risø, 1991, pp. 241–246.
[31] G. Garcés, P. Pérez, P. Adeva, Scr. Mater. 52 (2005) 615–619.
[32] T.W. Clyne, P.J. Withers, An Introduction to Metal Matrix Composites, Cambridge University Press, Cambridge, 1993, pp. 44–70.
[33] I. Karaman, H. Sehitoglu, A.J. Beaudoin, Y.I. Chumlyakov, H.J. Maier, C.N. Tomé, Acta Mater. 48 (2000) 2031–2047.
[34] Z.S. Basinski, M.S. Szczerba, M. Niewczas, J.D. Embury, S.J. Basinski, Rev. Metall. 94 (1997) 1037–1043.
[35] R. Armstrong, L. Codd, R.M. Douthwaite, N.J. Petch, Philos. Magn. 7 (1962) 45–69.
[36] F. Lavrentev, Mater. Sci. Eng. 46 (1980) 191–208.
[37] H.J. Frost, M.F. Ashby, Deformation-Mechanism Maps: The Plasticity and Creep of Metals and Ceramics, Pergamon, Oxford, 1982, p. 44.
[38] W.S. Miller, F.J. Humphreys, Scr. Metall. Mater. 25 (1991) 33–38.
[39] F.E. Hauser, P.R. Landon, J.E. Dorn, AIME Trans. 206 (1956) 589–593.
[40] P. Andersson, C.H. Cáceres, J. Koike, Mater. Sci. Forum 419–422 (2003) 123–128.
[41] R.J. Arsenault, M. Taya, Acta Metall. 35 (1987) 651–659.